LETTER TO THE EDITOR

ERULUS Is a Plasma Membrane-Localized Receptor-Like Kinase That Specifies Root Hair Growth by Maintaining Tip-Focused Cytoplasmic Calcium Oscillations[OPEN]

Root hairs are single-cell cylindrical projections that expand the effective radius of the root. In doing so, they play crucial roles in the uptake of water and nutrients from the soil, especially under conditions in which such resources are limiting (Carminati et al., 2017). Root hairs expand by tip growth, a process that involves the targeted delivery and secretion of vesicles to the cell apex. As a result, root hairs attain lengths that are several times their widths (Chebli et al., 2013). In tip-growing cells, cargo transported by tip-targeted vesicles consist of an assortment of carbohydrate precursors that are needed for the assembly and re-modeling of the apical cell wall (Gu and Nielsen, 2013). Research spanning several decades has led to the identification of multiple components of the tip growth machinery including protein modulators of cytoskeletal organization, membrane trafficking, cytoplasmic calcium ($[Ca^{2+}]_{cyt}$) signaling, and phosphoinositide metabolism (Cole and Fowler, 2006; Rounds and Bezanilla, 2013).

In recent years, plant malectin-like receptor kinases, also known as *Catharanthus roseus* receptor-like kinases (CrRLK1Ls; Franck et al., 2018), have been shown to regulate tip growth in root hairs and pollen tubes (Duan et al., 2010; Bai et al., 2014; Haruta et al., 2014; Ge et al., 2017; Schoenaers et al., 2018). In one noteworthy study, Bai et al. (2014) reported that a CrRLK1L, which they named $[Ca^{2+}]_{cyt}$-associated protein kinase 1 (CAP1), modulates root hair growth by maintaining ammonium (NH_4^+) homeostasis. CAP1 is also known as ERULUS (ERU), named after the son of FERONIA

(FER), a widely studied member of the CrRLK1L family (Haruta et al., 2014). In *Arabidopsis thaliana*, *cap1/eru* loss-of-function mutants have short and irregularly shaped root hairs consistent with a role of CAP1/ERU as a positive regulator of root hair growth (Bai et al., 2014; Haruta et al., 2014; Schoenaers et al., 2018). Bai et al. (2014) proposed a model wherein CAP1/ERU functions in maintaining root hair growth under high NH_4^+ environments by sensing cytoplasmic NH_4^+. Sensing of cytoplasmic NH_4^+ by CAP1/ERU then triggers signaling events that lead to NH_4^+ sequestration into the vacuole, making it less toxic to the cell. The model postulates that toxic levels of NH_4^+ accumulate in the cytoplasm of *cap1/eru* loss-of-function mutants, resulting in the disappearance of tip-focused $[Ca^{2+}]_{cyt}$ gradients, and because of this lack of tip-focused $[Ca^{2+}]_{cyt}$ gradients, their root hairs cease to expand (Bai et al., 2014). In this letter, we question the proposed role of CAP1/ERU in NH_4^+ homeostasis based on our studies of a new *eru-3* mutant allele, showing that CAP1/ERU is instead localized to the plasma membrane (PM) and its function is linked to tip-focused $[Ca^{2+}]_{cyt}$ oscillations. This is further supported by recent work on the *eru-2* mutant by Schoenaers et al. (2018), as described below.

CAP1/ERU IS A PM-LOCALIZED PROTEIN

A major result used to support the CAP1/ERU-NH_4^+ homeostasis model was the observation that a CAP1/ERU-GFP fusion localized to the tonoplast. According to the model, the tonoplast-localized CAP1/ERU is what senses cytoplasmic NH_4^+, resulting in its compartmentalization into the vacuole (Bai et al., 2014).

We independently isolated the recessive *eru-3* mutant in a forward-genetic screen for root hair mutants that resembled wild-type root hairs treated with low concentrations of the actin-disrupting compound latrunculin B. Here, we refer to our mutant as *eru-3* following the nomenclature of Haruta et al. (2014), in which two mutant alleles of *eru* were first described as *eru-1* and *eru-2*. The *cap1* mutant (SALK_083442) studied by Bai et al. (2014) is similar to *eru-2*; therefore, we refer to it here as *cap1/eru-2* (Figure 1A). When we expressed an *ERU-GFP* construct under the control of the constitutive *UBIQUITIN10* (*UBQ10*) promoter (*UBQ10:ERU-GFP*) in the *eru-3* mutants, their root hairs were restored to wild-type lengths, indicating that the fusion protein was functional (Figures 1B and 1C).

We found that instead of localizing to the root hair tonoplast, ERU-GFP marked the PM at the site of root hair bulges. As root hairs transitioned to rapid tip growth, the ERU-GFP signal intensified and formed a diffuse fluorescent cap at the root hair apex (Figure 1D). Distal to the root hair tip, ERU-GFP decorated distinct and dynamic puncta that were reminiscent of post-Golgi and endocytic vesicles (Figure 1D). As root hairs matured and ceased growth, the intensity of ERU-GFP at the tip declined (Figure 1D). Time-course and correlation analyses revealed that tip-directed accumulation of ERU-GFP was most intense in root hairs that grew rapidly (Figures 1E and 1F), supporting the role of ERU as a positive regulator of root hair tip growth.

It is important to note that Bai et al. (2014) used transient expression of a CAP1/ERU-GFP fusion in protoplasts and onion epidermal cells to conclude that it localized to the tonoplast, and the functionality of their CAP1/ERU-GFP construct was not validated in root hairs. It is
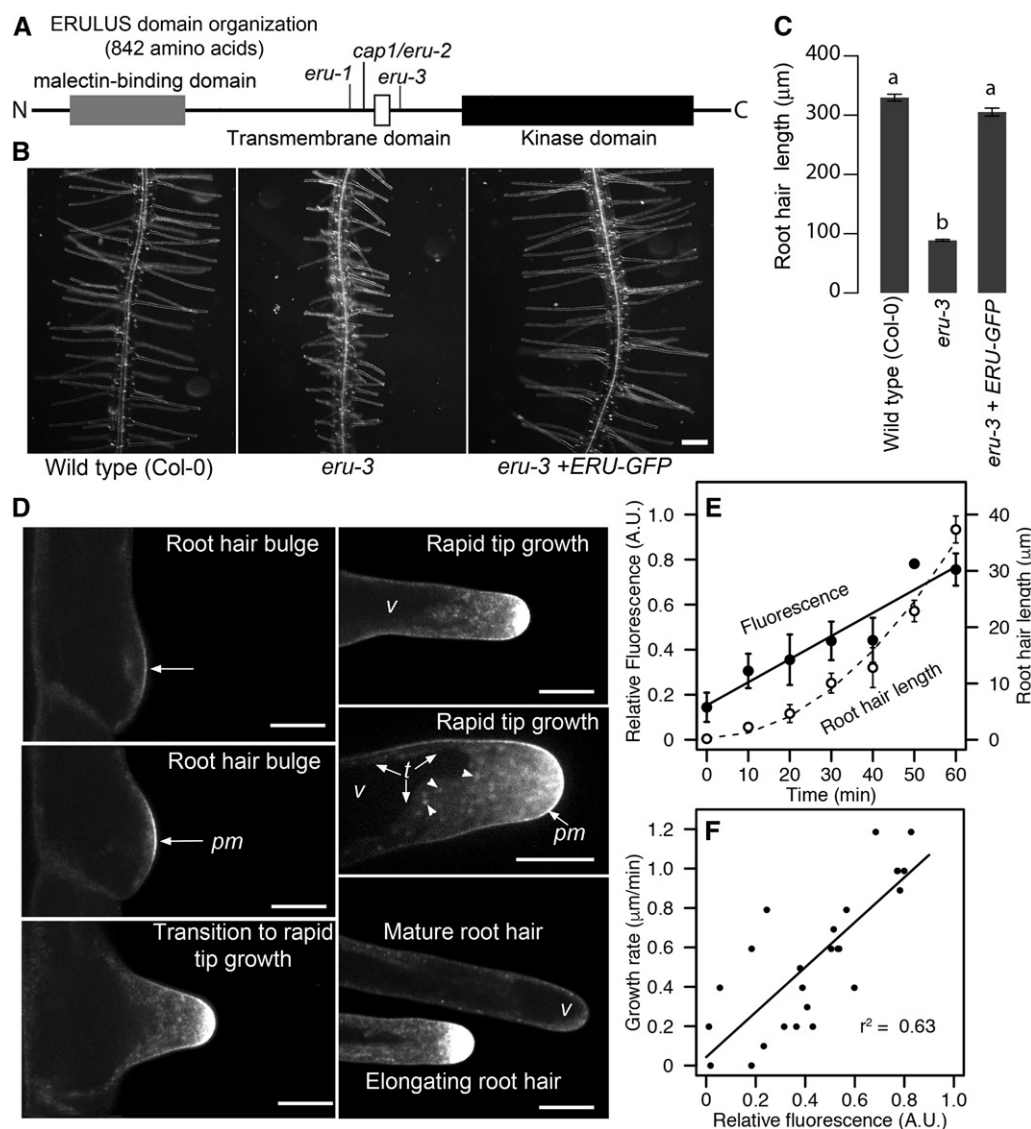
Figure 1. A Functional ERU-GFP Fusion Localizes to the PM and Post-Golgi/Endocytic Vesicles at the Root Hair Tip.

(A) Schematic diagram of the domain organization of the ERU protein. Relative positions of T-DNA insertions of *eru-1*, *cap1/eru-2*, and *eru-3* are indicated as vertical lines.

(B) and **(C)** *UBQ10:ERU-GFP* complements the short root hair phenotypes of *eru-3*. Statistical significance for root hair length was determined by one-way ANOVA. Means ± SE (n = 215 for Col-0, 195 for *eru-3*, and 264 for *eru-3+ERU-GFP* root hairs from five independent 4-d-old seedlings per genotype). Different letters indicate significant difference (Tukey's test, P < 0.001). Bar = 100 μm.

(D) Localization of ERU-GFP in root hairs at various stages of development. *pm*, PM; *v*, vacuole; *t*, tonoplast. In addition to the PM, ERU-GFP marks distinct puncta (arrowheads) in root hairs undergoing rapid tip growth. Bars = 10 μm.

(E) Double *y* axis graph showing that fluorescence of ERU-GFP intensifies as root hairs transition to rapid tip growth. Relative fluorescence and root hair length were measured every 10 min. Mean ± SE (n = 4 root hairs from four independent 4-d-old seedlings).

(F) Scatterplot showing that fluorescence of ERU-GFP is positively correlated with growth rate of root hairs (P < 2.2×10^{-6}). The same data were plotted in **(E)** and **(F)**. See detailed methods in supplemental data.

possible that their CAP1/ERU-GFP was mislocalized because it was expressed in cell types (i.e., leaf protoplasts and onion epidermal cells) in which ERU is not typically found. We attempted to express ERU-GFP in the *eru-3* mutant under the control of the native *ERU* promoter (*ERU$_{pro}$*) consisting of 626 bp upstream of the *ERU* gene. Unfortunately, we were unable to recover *ERU$_{pro}$:ERU-GFP* lines. However, it was recently reported that a 2529-bp sequence that included the *ERU* promoter coupled to the *ERU* coding and *GFP* sequence (*ERUp:ERU-GFP*) complemented *cap1/eru-2* root hairs
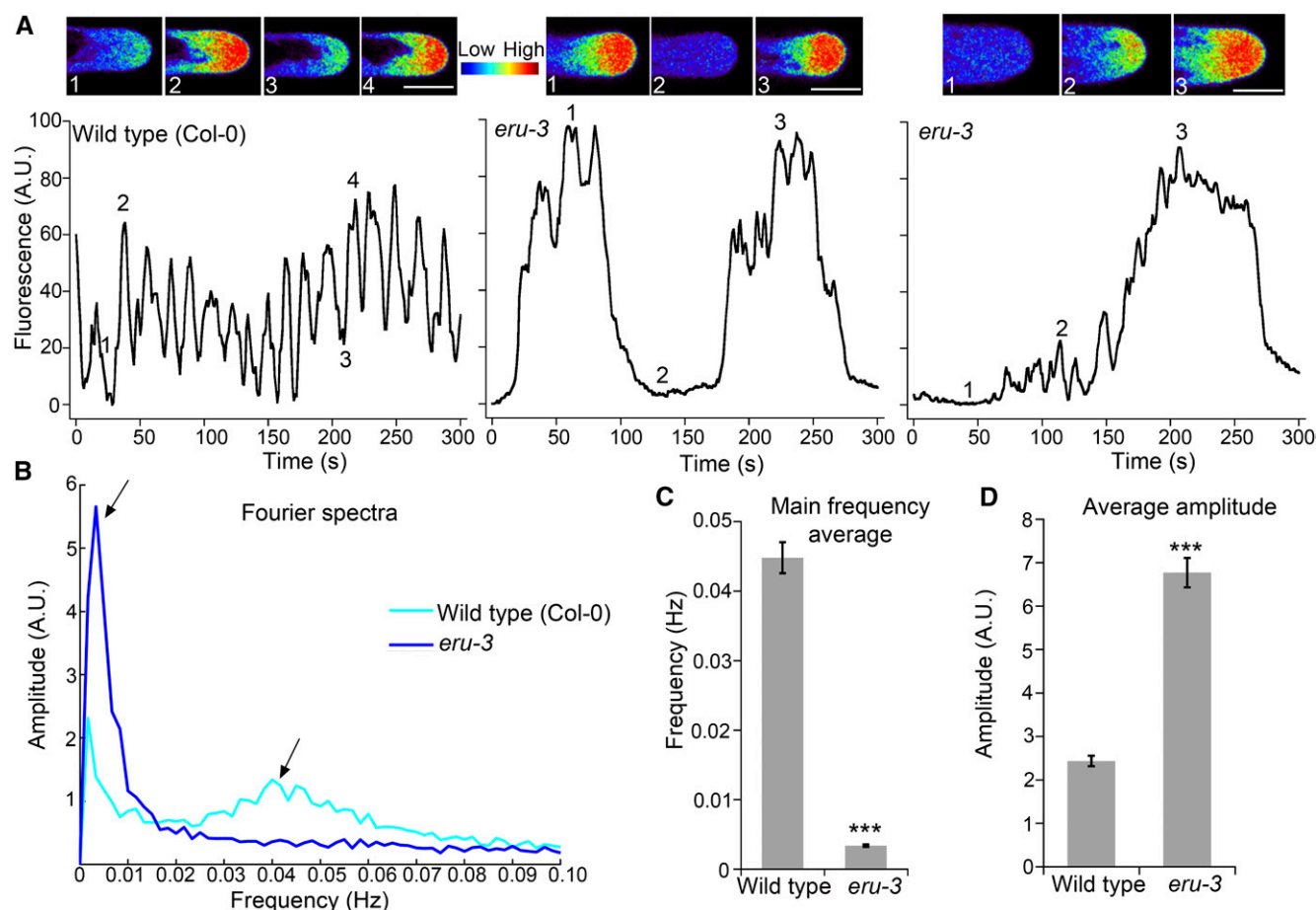
Figure 2. ERU Functions in Maintaining Normal Tip-Focused $[Ca^{2+}]_{cyt}$ in Root Hairs.

(A) Representative heat maps of the root hair apex and normalized oscillograms of one wild-type and two *eru-3* mutants. Numbers in the pseudocolored images correspond to indicated positions on the oscillogram. The entire time-lapse sequence corresponding to each oscillogram can be seen in Supplemental Movie 1, with red indicating the highest $[Ca^{2+}]_{cyt}$-dependent fluorescence. Bars = 10 μm.

(B) Fourier spectra corresponding to wild-type and *eru-3* root hair tip-focused $[Ca^{2+}]_{cyt}$ oscillations shown on the rightmost panels of **(A)**. Main oscillation frequencies for each genotype are indicated by the arrows.

(C) and **(D)** Bar graphs showing the average frequency and amplitude of the main Fourier peaks for wild-type and *eru-3* root hairs. Means ± SE (*n* = 31 wild-type and 36 *eru-3* root hairs from 10 independent 5-d-old seedlings per genotype). ***P < 0.0001, Student's *t* test. See detailed methods in supplemental data.

(Schoenaers et al., 2018). This group found that expressed ERU-GFP localized to root hairs in a similar manner as our constitutively expressed ERU-GFP, further supporting our conclusion that the PM is where the ERU protein resides.

CAP1/ERU FUNCTION IS LINKED TO CYTOPLASMIC CALCIUM OSCILLATIONS

Another major result of Bai et al. (2014) that we address in this letter is their finding that root hairs of *cap1/eru* loss-of-function mutants appeared to lack tip-focused $[Ca^{2+}]_{cyt}$ gradients. We feel that it is important to address these results because they provide an example of how $[Ca^{2+}]_{cyt}$ imaging data on root hairs can be misinterpreted. For these experiments, it is critical to note that root hair growth ceases when the large central vacuole protrudes toward the cell apex (Grierson et al., 2014). Furthermore, mature, nongrowing root hairs in which the vacuole protrudes to the apex have been shown to lack $[Ca^{2+}]_{cyt}$ gradients (Wymer et al., 1997). The images of *cap1/eru-2*

root hairs that Bai et al. (2014) presented as the basis for extracting their $[Ca^{2+}]_{cyt}$ data (Figures 2A and 3C in Bai et al. [2014]) clearly showed the vacuole protruding to the apex. Based on the above observations, we would not expect to find $[Ca^{2+}]_{cyt}$ gradients in such root hairs. We expressed the intensiometric $[Ca^{2+}]_{cyt}$ reporter G-CAMP3 (Tian et al., 2009) in *eru-3* to assess if their root hairs lacked a $[Ca^{2+}]_{cyt}$ gradient. We were careful to sample $[Ca^{2+}]_{cyt}$ only in root hairs that had a dense cytoplasm at the cell apex.

In contrast to the results of Bai et al. (2014), we found that *eru-3* root hairs that still had a substantial cytoplasm at the apex did not lack tip-focused $[Ca^{2+}]_{cyt}$ gradients. These *eru-3* root hairs were still elongating, albeit at a significantly reduced rate when compared with the wild type (~0.20 µm/min for *eru-3* versus 1 µm/min for the wild type). However, we did observe that patterns of tip $[Ca^{2+}]_{cyt}$ oscillations in these slow growing *eru-3* root hairs were compromised. Compared with the wild type, root hairs of *eru-3* had more prolonged periods of elevated tip-focused $[Ca^{2+}]_{cyt}$ followed by longer periods of dampened $[Ca^{2+}]_{cyt}$ (Figures 2A to 2C; Supplemental Movie 1). Quantitative analysis of $[Ca^{2+}]_{cyt}$ following the fast Fourier transform methods described by Schoenaers et al. (2018) showed that *eru-3* displayed low frequency $[Ca^{2+}]_{cyt}$ oscillations. The main frequency of $[Ca^{2+}]_{cyt}$ oscillations in *eru-3* root hairs was 0.003 ± 0.0002 Hz compared with 0.044 ± 0.0184 Hz in the wild type (Figure 2D). Furthermore, the amplitude of $[Ca^{2+}]_{cyt}$ oscillation at the tips of *eru-3* was ~3-fold higher than the wild type (Figure 2E). These results are in agreement with findings of Schoenaers et al. (2018) in which they showed decreased frequency and increased amplitude of pectin Ca^{2+} binding site oscillations in *cap1/eru-2* root hairs. It is clear from our results that ERU is important for normal tip-focused $[Ca^{2+}]_{cyt}$ oscillations, a process that is crucial for sustained root hair growth (Monshausen et al., 2008). Mechanistic links between PM-localized ERU and the maintenance of $[Ca^{2+}]_{cyt}$ oscillations are unknown. However, demonstrating the true nature of tip-focused $[Ca^{2+}]_{cyt}$ defects in *eru-3* root hairs enables the development of more accurate models that could be tested in the future to explain how ERU modulates tip growth.

In light of the ERU localization data presented here and those reported by Schoenaers et al. (2018), the model by Bai et al. (2014), proposing that tonoplast-based NH_4^+ signaling is the major driver for ERU-mediated tip-focused $[Ca^{2+}]_{cyt}$ oscillations and root hair growth, needs reexamination. Other CrRLK1Ls, such as FER, THESEUS1, HERCULES1, ANXUR, and BUDDHA's PAPER SEAL, have all been shown to localize to the PM (Escobar-Restrepo et al., 2007; Hématy et al., 2007; Boisson-Dernier et al., 2009; Guo et al., 2009; Miyazaki et al., 2009; Duan et al., 2010; Ge et al., 2017). Our results and those of Schoenaers et al. (2018) clearly demonstrate that ERU is also a PM-localized CrRLK1L and should no longer be referred to as a vacuolar membrane-localized protein.

Supplemental Data

Supplemental Methods. Identification of the *eru-3* mutant, *UBQ10:ERU-GFP* and *UBQ10:G-CAMP3* constructs, and live-cell microscopy of root hairs.

Supplemental Movie 1. Time-lapse sequences of wild-type and *eru-3* tip $[Ca^{2+}]_{cyt}$ oscillations.

Supplemental Movie Legend.

Taegun Kwon
Noble Research Institute
Ardmore, Oklahoma 73401
eblancaflor@noble.org
ORCID ID: 0000-0002-0205-8535

J. Alan Sparks
Noble Research Institute
Ardmore, Oklahoma 73401
ORCID ID: 0000-0002-4492-9810

Fuqi Liao
Noble Research Institute
Ardmore, Oklahoma 73401
ORCID ID: 0000-0002-3740-2949

Elison B. Blancaflor
Noble Research Institute
Ardmore, Oklahoma 73401
ORCID ID: 0000-0001-6115-9670

ACKNOWLEDGMENTS

AUTHOR CONTRIBUTIONS

T.K. and E.B.B. drafted the manuscript. T.K. and J.A.S. generated and analyzed plants expressing ERU-GFP and G-CAMP. T.K., J.A.S., and E.B.B. performed root hair confocal imaging and forward genetic screens. F.L. quantified and interpreted $[Ca^{2+}]_{cyt}$ oscillations using fast Fourier transform methods.

REFERENCES

Bai, L., Ma, X., Zhang, G., Song, S., Zhou, Y., Gao, L., Miao, Y., and Song, C.-P. (2014). A receptor-like kinase mediates ammonium homeostasis and is important for the polar growth of root hairs in *Arabidopsis*. Plant Cell **26:** 1497–1511.

Boisson-Dernier, A., Roy, S., Kritsas, K., Grobei, M.A., Jaciubek, M., Schroeder, J.I., and Grossniklaus, U. (2009). Disruption of the pollen-expressed *FERONIA* homologs *ANXUR1* and *ANXUR2* triggers pollen tube discharge. Development **136:** 3279–3288.

Carminati, A., Passioura, J.B., Zarebanadkouki, M., Ahmed, M.A., Ryan, P.R., Watt, M., and Delhaize, E. (2017). Root hairs enable high transpiration rates in drying soils. New Phytol. **216:** 771–781.

Chebli, Y., Kroeger, J., and Geitmann, A. (2013). Transport logistics in pollen tubes. Mol. Plant **6:** 1037–1052.

Cole, R.A., and Fowler, J.E. (2006). Polarized growth: maintaining focus on the tip. Curr. Opin. Plant Biol. **9:** 579–588.

Duan, Q., Kita, D., Li, C., Cheung, A.Y., and Wu, H.-M. (2010). FERONIA receptor-like kinase regulates RHO GTPase signaling of root hair development. Proc. Natl. Acad. Sci. USA **107:** 17821–17826.

Escobar-Restrepo, J.-M., Huck, N., Kessler, S., Gagliardini, V., Gheyselinck, J., Yang, W.-C., and Grossniklaus, U. (2007). The FERONIA receptor-like kinase mediates male-female interactions during pollen tube reception. Science **317:** 656–660.

Franck, C.M., Westermann, J., and Boisson-Dernier, A. (2018). Plant malectin-like receptor kinases: from cell wall integrity to immunity and beyond. Annu. Rev. Plant Biol. **69:** 301–328.

Ge, Z., et al. (2017). *Arabidopsis* pollen tube integrity and sperm release are regulated by RALF-mediated signaling. Science **358:** 1596–1600.

Grierson, C., Nielsen, E., Ketelaarc, T., and Schiefelbein, J. (2014). Root hairs. The Arabidopsis Book **12:** e0172, doi/10.1199/tab.0172.

Gu, F., and Nielsen, E. (2013). Targeting and regulation of cell wall synthesis during tip growth in plants. J. Integr. Plant Biol. **55:** 835–846.

Guo, H., Li, L., Ye, H., Yu, X., Algreen, A., and Yin, Y. (2009). Three related receptor-like kinases are required for optimal cell elongation in *Arabidopsis thaliana*. Proc. Natl. Acad. Sci. USA **106:** 7648–7653.

Haruta, M., Sabat, G., Stecker, K., Minkoff, B.B., and Sussman, M.R. (2014). A peptide hormone and its receptor protein kinase regulate plant cell expansion. Science **343:** 408–411.

Hématy, K., Sado, P.-E., Van Tuinen, A., Rochange, S., Desnos, T., Balzergue, S., Pelletier, S., Renou, J.-P., and Höfte, H. (2007). A receptor-like kinase mediates the response of *Arabidopsis* cells to the inhibition of cellulose synthesis. Curr. Biol. **17:** 922–931.

Miyazaki, S., Murata, T., Sakurai-Ozato, N., Kubo, M., Demura, T., Fukuda, H., and Hasebe, M. (2009). *ANXUR1* and *2*, sister genes to *FERONIA/SIRENE*, are male factors for coordinated fertilization. Curr. Biol. **19:** 1327–1331.

Monshausen, G.B., Messerli, M.A., and Gilroy, S. (2008). Imaging of the Yellow Cameleon 3.6 indicator reveals that elevations in cytosolic Ca^{2+} follow oscillating increases in growth in root hairs of *Arabidopsis.* Plant Physiol. **147:** 1690–1698.

Rounds, C.M., and Bezanilla, M. (2013). Growth mechanisms in tip-growing plant cells. Annu. Rev. Plant Biol. **64:** 243–265.

Schoenaers, S., et al. (2018). The auxin-regulated CrRLK1L kinase ERULUS controls cell wall composition during root hair tip growth. Curr. Biol. **28:** 722–732.

Tian, L., et al. (2009). Imaging neural activity in worms, flies and mice with improved GCaMP calcium indicators. Nat. Methods **6:** 875–881.

Wymer, C.L., Bibikova, T.N., and Gilroy, S. (1997). Cytoplasmic free calcium distributions during the development of root hairs of *Arabidopsis thaliana.* Plant J. **12:** 427–439.